JOURNAL OF THEORETICAL
AND APPLIED MECHANICS
42, 4, pp. 927-944, Warsaw 2004

BIOMECHANICAL MODELLING FOR WHOLE BODY MOTION USING NATURAL COORDINATES

Adam Czaplicki

Academy of Physical Education in Warsaw, External Faculty of Physical Education in Biala Podlaska, Department of Biomechanics, Poland; e-mail: czaplicki@poczta.onet.pl

Miguel T. Silva
Jorge C. Ambrósio

IDMEC – Institute of Mechanical Engineering, Technical University of Lisbon, Portugal
e-mail: pcms@mail.ist.utl.pt; jorge@dem.ist.utl.pt

The study of spatial human movements requires the development and use of a three-dimensional model. The model proposed here has 44 degrees-of-freedom and it is described using natural coordinates, which do not require an explicit definition of rotation coordinates. The biomechanical model consists of 16 anatomical segments composed of 33 rigid bodies. Joint actuators are introduced into equations of motion of the multibody model by means of kinematic driver constraints in order to reflect the effect of the muscle forces about each anatomical joint. After associating a Lagrange multiplier to each joint actuator, the torques that represent muscle forces become coupled with the biomechanical model through the Jacobian matrix of the underlying multibody system. The developed model is applied to identify net torques and reaction forces at the anatomical joints in application cases that include the take-off to aerial trajectories and standing backwards somersault.

Key words: biomechanical model, multibody dynamics, inverse dynamics, internal forces

1. Introduction

The natural coordinates were first proposed by Jalón *et al.* (1986) and described later in detail by Jalón and Bayo (1994). They provide a natural framework for the description of complete spatial motion of multibody systems without using rotation coordinates explicitly. Not only these coordinates lead to very efficient numerical models but also there is a direct connection between the coordinates defining the bodies and the anatomical landmarks associated to kinematic data acquisition typical to biomechanical modelling. Despite the fact that the natural coordinates are commonly used to investigate different types of mechanical systems, they are sporadically applied to biomechanics as proposed by Celigüeta (1996), Silva *et al.* (1997), Silva and Ambrósio (2002), and Ambrósio *et al.* (2001). Therefore, one of the purposes of this work is to demonstrate that the modelling in biomechanics by means of natural coordinates is not only efficient and attractive but also a natural way to map the body anatomical landmarks into coordinates defining the biomechanical system.

The number of natural coordinates used to represent a biomechanical model is always larger than its number of degrees-of-freedom, which means that they are related by proper algebraic constraint equations. These are usually nonlinear and play a major role in the kinematic and dynamic analysis of multibody systems. The number of independent algebraic constraint equations is equal to the difference between the number of natural coordinates and the number of degrees-of-freedom of a system. There are some aspects in which a set of natural coordinates is advantageous. First, the whole multibody system is defined directly in the global reference frame. Second, natural coordinates are usually defined at the joints of the system and shared by adjacent bodies, which reduces the total number of coordinates required to represent the model and considerably simplifies the definition of the joint constraint equations. Third, with natural coordinates the constraint equations, that arise from rigid body and joint conditions, are linear or quadratic. This means that their contribution to the Jacobian matrix of the constraints is a constant or linear function of the natural coordinates, which leads to efficient numerical implementations.

The aim of this paper is to present a general purpose methodology for the three-dimensional modelling in biomechanics. The approach is based on natural coordinates, and it focuses on the identification of internal reaction forces and net torques at anatomical joints of an individual performing selected motor tasks. Two different human activities have been chosen to demonstrate the method offered: the take-off for a jump and the standing backwards somersault. The selected jump is being very often preformed when passing natural obstacles like puddles or ditches, and it is undoubtedly a frequent human activity. Many researches have so far conducted analyses of long jumps (e.g., Hay, 1993; Lees *et al.*, 1994) and of other related motor task like vertical jumping (e.g., Pandy *et al.*, 1990, 1992; Bobbert and Schenau, 1988; Selbie and

Caldwell, 1996; Eberhard *et al.*, 1999). However, in the case of the specified jump, these articles can be helpful in a very limited way since they are either descriptive by nature or the results reported concern two-dimensional models only. Numerous standing backwards somersault analyses deal mostly with the methodology of learning this stunt neglecting its mechanical aspects (e.g., Mieczkowski, 1982). The quantitative description of the standing backwards somersault is important for both cognitive and practical reasons, leading to better understanding of the athlete movements and forms a basis for more conscious mastering of the evolution of the somersault technique. In the process of studying the standing backwards somersault in terms of the biomechanical analysis, a three-dimensional methodology is proposed in this work and is demonstrated in a movement of the human body that leads to a change in space positions of anatomical segments by a complete revolution by 360 degrees, emphasizing the robustness of the methods adopted.

2. Biomechanical model

The study presented here uses the biomechanical model shown in Fig. 1a, which consists of 16 anatomical segments. The biomechanical model is described by natural coordinates that are used to construct its kinematic structure made of 33 rigid bodies branching from the pelvis in open chain linkages (Silva and Ambrósio, 2002). The rigid bodies that form the neck, arms, forearms, thighs, shanks, upper torso (numbered in Fig. 1b from 19 to 25) and the lower torso (numbers 6, 7, 8) are defined by the Cartesian coordinates of two points and one unit vector each. The hands, feet and head are defined by the coordinates of three points and one unit vector. The first type of the rigid body has a simpler kinematic structure but generates a non-constant mass matrix in the equations of motion of the system. The second type of the rigid body has a more complex kinematic structure but generates a constant mass matrix (Jalón and Bayo, 1994). The complete set of rigid bodies is described by means of 25 points and 22 unit vectors, accounting a total number of 141 natural coordinates.

The most common way of modelling the joints in the natural coordinates environment, corresponding to the sharing points and vectors among the adjacent segments, is depicted in Fig. 2.

The kinematic structure of the biomechanical model, shown in Fig. 1c, is worth noticing as it suggests a more detailed discussion. The calculation of the internal joint reactions is usually very important from the biomechanical

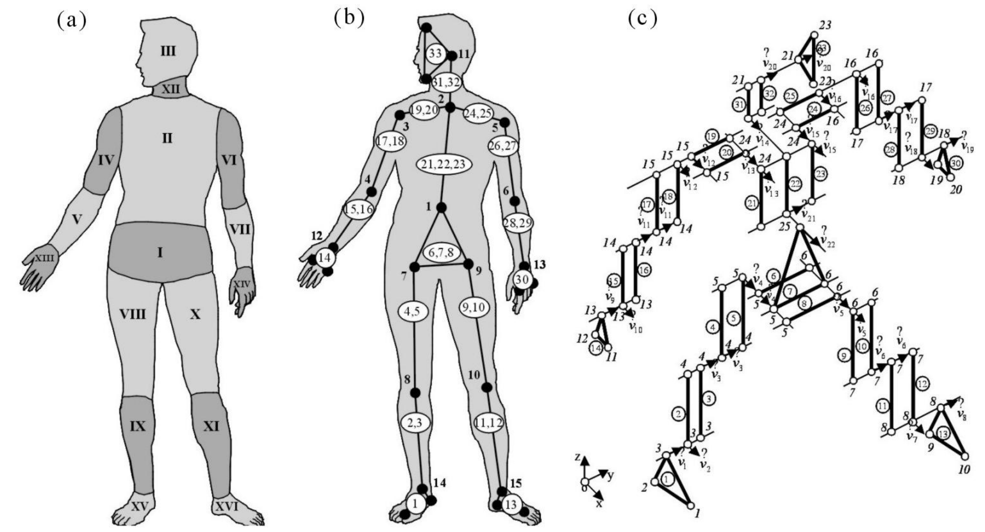

Fig. 1. Biomechanical model. (a) Representation of sixteen anatomical segments; (b) the structure of thirty three rigid bodies (with body numbers inside circles) used to represent the sixteen anatomical segments, and fifteen kinematic joints (with the joint numbers in bold); (c) an exploded view of the kinematic structure of the biomechanical model with indication of the points (represented in italic) and unit vectors

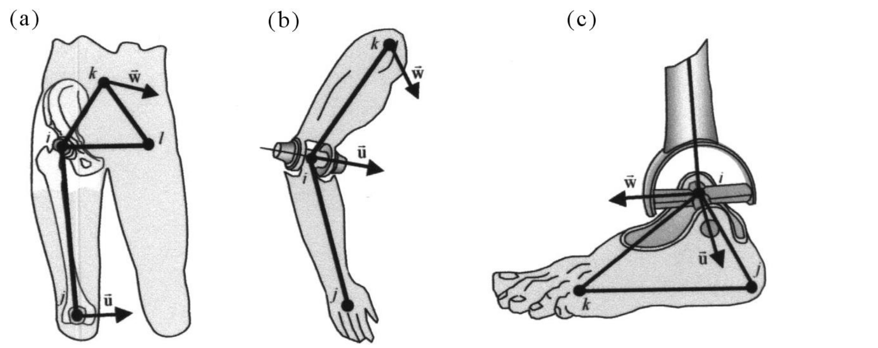

Fig. 2. The model of anatomical joints with natural coordinates: (a) the spherical joint for the hip; (b) the revolute joint for the elbow; (c) the universal joint for the ankle

standpoint. To calculate their anterior- posterior, medial-lateral and vertical components, all the kinematic joint constraints must be explicitly defined. This is achieved by introducing additional rigid bodies, points and unit vectors at the joints that are physically the same but mathematically distinguishable (Silva, 2003). As a result, the kinematic structure of the biomechanical model becomes more complex and the biomechanical model is provided with revolute and universal joints only, as represented in Fig. 1c. The universal joints are located in the ankle, in the radioulnar articulations, between the 12th thoracic and 1st lumbar vertebrae (designated by lower-upper torso joint) and between the 7th cervical and 1st thoracic vertebrae (referred to as the upper torso-neck joint). Since most of the joints are defined naturally by the sharing points and vectors between the contiguous segments, there is a total number of 97 non-redundant kinematic constraints only. The model has 44 degrees of freedom that correspond to 38 rotations about the revolute and universal joints, and 6 degrees-of-freedom associated with the pelvis, which is treated as the base body. The degrees-of-freedom of the biomechanical model proposed are numbered in Fig. 3a.

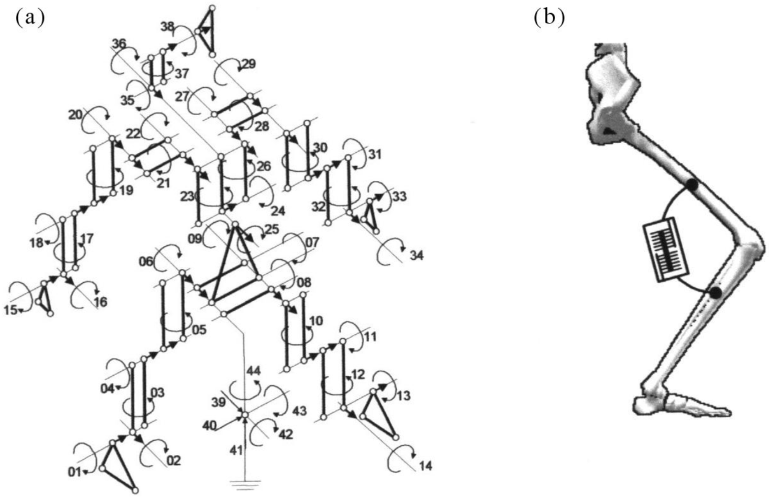

Fig. 3. (a) Degrees of freedom of the biomechanical model; (b) the joint actuator driving the knee joint in the sagittal plane

One of the forms of calculating internal net torques at the joints of the biomechanical model is to assume that each degree-of-freedom is driven by an adequate joint actuator, such as the one depicted in Fig. 3b. Joint actuators are introduced into equations of motion of the biomechanical model by means of kinematic driver constraints of the scalar product type, which are described in Table 1.

The body segment parameters for the biomechanical model, which include the body mass, principal moments of inertia, segment lengths, and location of the center of mass of each segment with respect to the proximal joint, are estimated from the data reported by Laananen *et al.* (1983), Laananen (1991) and Zatsiorsky (1998). All these parameters are scaled according to the subject height and mass using the procedures proposed by Laananen (1991).

3. Multibody formulation

Individual rigid bodies of the biomechanical model are described by means of a set of natural coordinates that is composed of the Cartesian coordinates of several points and unit vectors located at the joints and segment extremities. The vector of generalized coordinates of the whole biomechanical model is denoted by

$$\boldsymbol{q} = [q_1, q_2, \dots, q_n]^\top \tag{3.1}$$

where $n = 3(np + nv)$ is the total number of natural coordinates and np and nv are the total number of points and unit vectors of the model, respectively. The number of natural coordinates is always higher than the number of degrees-of-freedom of the system, which means that some kinematic constraint equations need to be added to unequivocally define the kinematic structure and topology of the biomechanical model. In addition to the joint and driving constraints, there are also rigid body constraints utilized in the multibody approach presented. They express physical properties of rigid bodies such as constant distance between two points, constant angle between two segments or constant length of a unit vector. The latter condition implies the normalization constraint $a_x^2 + a_y^2 + a_z^2 = 1$ on the coordinates of the unit vector $a = [a_x, a_y, a_z]^\top$. The physical interpretation of a Lagrange multiplier associated with this constraint when performing the inverse dynamic analysis is an axial pair of forces applied at the extremities of the unit vector. The rigid body and driving constraints may be represented by the scalar product equation

$$\boldsymbol{\Phi}^{sp}(\boldsymbol{q}, t) = \boldsymbol{v}^\top \boldsymbol{u} - L_v L_u \cos(\langle \boldsymbol{v}, \boldsymbol{u} \rangle(t)) = \boldsymbol{0} \tag{3.2}$$

where $\boldsymbol{v}$ and $\boldsymbol{u}$ are two generic vectors used in the definition of rigid bodies, L_v and L_u are their respective norms and $\langle \boldsymbol{v}, \boldsymbol{u} \rangle(t)$ is the angle between them, which may be time dependent. It is worth pointing out that the parameters (L_u, L_v and $\langle \boldsymbol{v}, \boldsymbol{u} \rangle(t)$) in Eq. (3.2) describe constraints imposed on $\boldsymbol{u}$ and $\boldsymbol{v}$. They have constant or varying values (for driving constraints) and are computed (for non-driving constraints) only once at the beginning of the analysis in the pre-processing phase. Equation (3.2) presents some innovative aspects when compared with the original formulation proposed by Jálon and Bayo (1994), since it comprises in a single analytical expression several kinematic constraints with different physical meanings, depending on the process of calculation of the vectors $\boldsymbol{v}$ and $\boldsymbol{u}$. Considering that $\boldsymbol{r}_i$, $\boldsymbol{r}_j$, $\boldsymbol{r}_k$ and $\boldsymbol{r}_l$ are the Cartesian coordinates of the points i, j, k and l, and that $\boldsymbol{a}$ and $\boldsymbol{b}$ are unit vectors, the most relevant kinematic constraints involving the scalar product and their physical meanings are presented in Table 1.

Table 1. Physical meanings of the scalar product constraints

Constraint description	$\boldsymbol{v}$	$\boldsymbol{u}$	L_v	L_u	$\langle \boldsymbol{v}, \boldsymbol{u} \rangle$	Graphical representation
Constant distance between points i and j	B_{ji}	B_{ji}	L_{ij}	L_{ij}	0	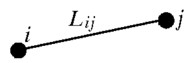
Unit module vector	$\boldsymbol{a}$	$\boldsymbol{a}$	1	1	0	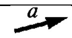
Constant angle between unit vectors $\boldsymbol{a}$ and $\boldsymbol{b}$	$\boldsymbol{a}$	$\boldsymbol{a}$	1	1	α	
Constant angle between segment $\boldsymbol{r}_{ij}$ and unit vector $\boldsymbol{a}$	B_{ji}	$\boldsymbol{a}$	L_{ij}	1	β	
Constant angle between segments $\boldsymbol{r}_{ij}$ and $\boldsymbol{r}_{kl}$	B_{ji}	B_{ik}	L_{ij}	L_{kl}	γ	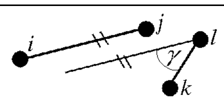
Rotational driver around revolute joint located in point i, using segments $\boldsymbol{r}_{ij}$ and $\boldsymbol{r}_{ik}$	B_{ji}	B_{ki}	L_{ij}	L_{ik}	ϕ	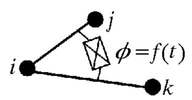

where $B_{ij} = (\boldsymbol{r}_i - \boldsymbol{r}_j)$ and $\phi = f(t)$.

With the natural coordinates, the constraint equations that arise from a rigid body and joint conditions are quadratic, so their Jacobian matrix is a linear function of the natural coordinates, which is very useful from the programming standpoint. In addition, Equation (3.2) may express rheonomic constraints when the angle $\langle \boldsymbol{v}, \boldsymbol{u} \rangle$ varies in time, which is used to define rotational driver actuators, such as the one presented in Fig. 3b. All constraint equations are assembled in a single vector denoted as

$$\boldsymbol{\Phi}(\boldsymbol{q}, t) = \boldsymbol{0} \tag{3.3}$$

The biomechanical model is implemented in a general purpose multibody code (Nikravesh, 1988; Haug, 1989; Schiehlen, 1997; Silva, 2003). The dynamic equations of motion for the model can be written in the generic form as

$$\mathbf{M}\ddot{\boldsymbol{q}} + \boldsymbol{\Phi}_q^\top \boldsymbol{\lambda} = \boldsymbol{g} \tag{3.4}$$

where $\mathbf{M}$ is the global mass matrix of the system, $\boldsymbol{\Phi}_q$ the Jacobian matrix of the constraints, $\ddot{\boldsymbol{q}}$ the vector of generalized accelerations, $\boldsymbol{g}$ the generalized force vector and $\boldsymbol{\lambda}$ the vector of Lagrange multipliers. Note that the product $\boldsymbol{\Phi}_q^\top \boldsymbol{\lambda}$ in Eq. (3.4) represents the joint reaction forces and the joint net moments. A unique vector $\boldsymbol{\lambda}$ is obtained when solving Eq. (3.4) during the inverse dynamics analysis. This is because the number of unknowns to calculate became equal to the number of equations of motion after introducing the driving constraints. It is worth pointing out that when solving the inverse dynamics problem one can obtain real values for the net torques (limited by the accuracy of the estimates of the angular accelerations only), but not real values for the reactions at the joints. Irrespective of methods applied, whether it is the Lagrange multipliers or conventional Newton-Euler approach, they do not take into account the contributions of individual muscle forces to the resultant joint reactions. Giving a graphic description of this fact, it is as if the biomechanical model was driven by torsional actuators located directly at the joints, instead of muscles. Nevertheless, the joint reactions computed this way are of great importance in the presence of transient external forces, and they can be easily adjusted after solving the individual muscle distribution problem at a particular joint.

4. Data acquisition

An adult male with the age of 23, height of 168 cm and a body mass of 68 kg, carried out several jumps and back somersaults. Among different trials, one of each activities was chosen as the most representative and was used in this work to illustrate the methodologies proposed. In all jumps, the force-plate data and the body motion kinematic data were synchronized and recorded simultaneously. The ground reaction forces were measured using a Kistler 9281B force platform at a sampling frequency at 1000 Hz, while the body motion was videotaped at 50 Hz by 4 synchronized cameras. The global reference frame was attached to the center of the force platform. The positions of the 23 anatomical points were used to reconstruct the motion. It is illustrated by two pictures shown in Fig. 4a, obtained during the beginning and the end of the take-off phase. The coordinates of all anatomical points projected in the video frames, were digitized manually. The DLT technique was used to calculate the spatial coordinates of the anatomical points (Abdel-Aziz and Karara, 1971). The raw data consisting on the spatial coordinates of the anatomical points was smoothed by means of a low-pass Butterworth 2nd order filter with zero-phase lag. Proper cut-off frequencies for every segment of the biomechanical model were chosen after performing a residual analysis (Winter, 1990). Such a residual analysis provides, for the type of motion under analysis, cut-off frequencies that range between 4 and 6 Hz. Taking into account the first investigated motor task, the average RMS differences (between raw and smoothed data) of 6.5 mm, 3.0 mm and 3.3 mm were estimated for the x, y, and z coordinates, respectively. The DLT procedure did not ensure constant lengths of the anatomical segments during all instants of time. Therefore, a technique that ensures the kinematic consistency of the motion data was applied to avoid further problems in the estimation of the net torques and reactions at the joints (Silva and Ambrósio, 2002). In the cited work, the time histories of the net torques at the ankle, knee and hip joints during gait obtained for consistent as well as non-consistent kinematic data were presented.

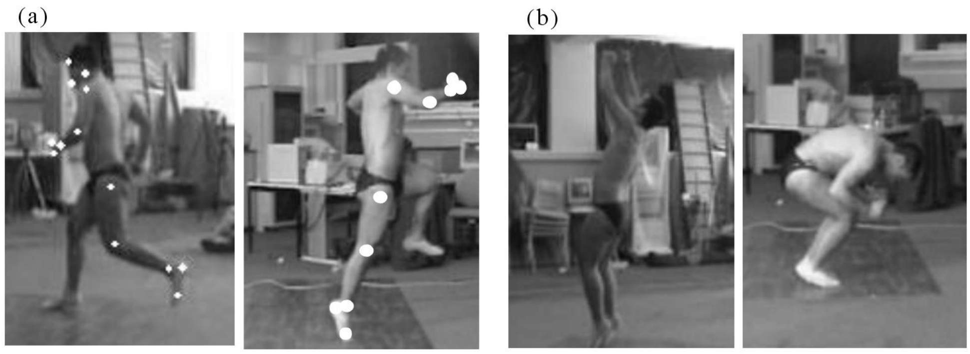

Fig. 4. Views from cameras 1 and 3; (a) long jump, white dots mark the positions of the 23 anatomical points; (b) standing backwards somersault, the end of take-off (left) and the beginning of landing (right)

5. Results

5.1. Long jump

The first step in order to apply the methods described is to acquire the force and kinematic data according to the data acquisition procedures proposed. The time characteristics of the measured ground reaction forces are shown in

Fig. 5. This force data presents significant differences from that obtained in the gait analysis not only due to the shapes of curves but also because of their magnitude. The maximum vertical reaction is almost four times larger than its equivalent in the gait and the peak value of the medial-lateral component is seven times higher than its analogue in the gait (Silva, 2003). It is worth noticing that the peak value of the anterior-posterior component of the force is larger than what is observed during jumps performed on a trampoline (Blajer and Czaplicki, 2003). An aliasing error during synchronization of the force plate data with the frequency of the video cameras is also visible.

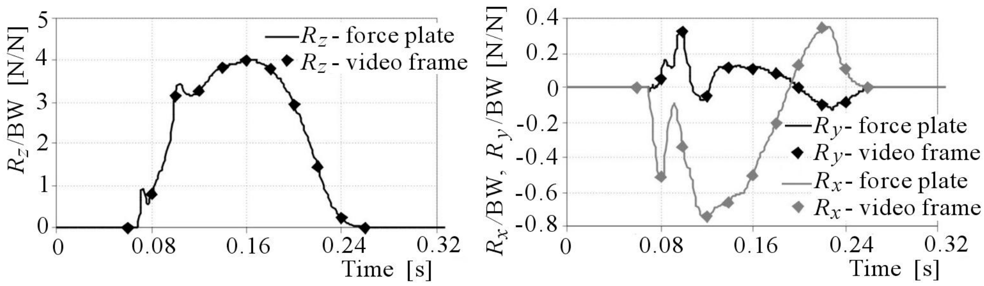

Fig. 5. Normalized vertical (R_z), anterior-posterior (R_x) and medial-lateral (R_y) components of the ground reaction force measured in the force platform. The markers denote the time instants for which there are video frames available. BW – body weight

The inverse dynamic analysis of the biomechanical model was firstly carried out to find the net moment of forces in the anatomical joints of the lower extremities. The results obtained in the inverse dynamic analysis of the jump are presented in Fig. 6. At the beginning of the trial, the jumper is in the air. Having the trunk in a forward-lean position, the jumper raises it to an upright position, which is achieved when the foot touches the ground. The net torque in the hip joint starts with positive values because the described movement requires the hamstrings and gluteus maximus to cooperate with each other. The large peak of the net torque in the hip joint, occurring at the beginning of the contact phase of the foot with the ground at $t = 0.08\,\mathrm{s}$, reflects the impact nature of the ground reaction force at that time. The net torque has a counterclockwise direction in the frontal plane, which means that the hip abductors, like glutei muscles and tensor fasciae latae, are active. The clockwise direction of the net torque in the sagittal plane in the hip joint together with the net torque oriented opposite in the knee joint indicate strong activity of vasti muscles. The ankle joint carries a considerable load during the support phase as a consequence of the stimulation of the triceps surae muscle generating powerful ankle plantarflexion in order to push the body forward and to prevent the shank bending down to the ground. Finally, there is a distinguishable net torque in the hip joint in the transversal plane at the beginning of the airborne phase, when the jumper starts moving his thighs towards the trunk. The activity of the hip adductors, gluteus maximus and iliopsoas muscles seems to ensure the medial rotation of the thigh.

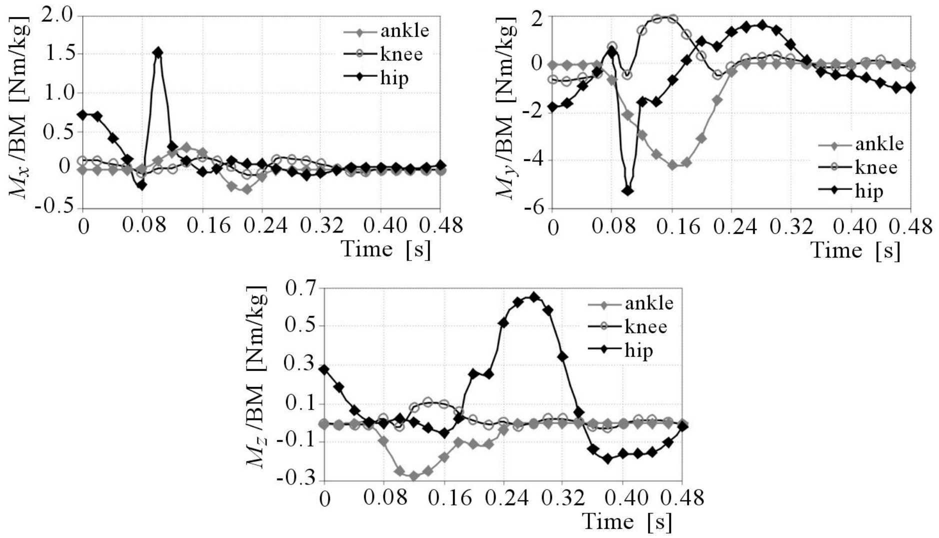

Fig. 6. Normalized net torques at the basic joints of the supporting leg of the jumper. BM – body mass

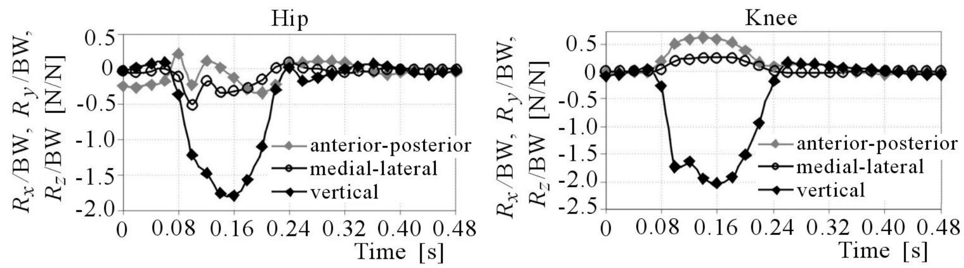

Fig. 7. Normalized reaction forces in the selected joints of the supporting leg during the jump

The joint reaction forces, associated with the type of analysis carried out, are depicted in Fig. 7. Note that using the joint torques to represent the muscle actions, the joint reaction forces are simply an approximation of the real forces, which can only be obtained with a complete muscle model. It is clearly visible, when comparing the curves presented in Fig. 5 and Fig. 7, considerable damping of the vertical reaction force between the ground and hip joint that ranges from 4 to 2 times the body weight. The anterior-posterior and the medial- lateral components of the resultant reaction in the knee and in the hip joint have practically opposite directions during the take-off phase of the jump, which means that the femur presses the knee joint anteriorly and medially, being simultaneously pressed posteriorly and laterally at the hip joint.

5.2. Standing backwards somersault

Having been an elite acrobat several years ago, the jumper performed the standing backwards somersault extremely well with a well developed technique, as represented in Fig. 4b. The upper and lower extremities were collateral during the stunt. The feet, having the same initial position in the anterior-posterior direction, were shifted only 0.8 cm apart from each other after landing. Because the external forces were measured using one force plate only, the correct technical performance of the jump allows assuming a symmetrical distribution of the ground reactions for the feet. The application point of the ground reaction was established on the heel-metatarsal line coinciding with the cast of the center of mass of the body on the force plate in the anterior-posterior direction.

The time characteristics of the measured ground reaction forces acquired are shown in Fig. 8. The largest value, of about 10 times the body weight at landing, is reached by the vertical ground reaction force. A decrease in the force, below the body weight during the first 0.5 s of the stunt due to a downward acceleration of the body performing a preparatory countermovement is also noticeable. This is followed by the overweight phase marked by a double humped pattern similar to that observed in high jumping (e.g., Pandy *et al.*, 1992). Peak magnitudes of the anterior-posterior component of the horizontal ground reaction lie in the vicinity of 3 times the body weight during landing. All presented characteristics distinctly emphasize the impact nature of the ground reaction during the beginning of the landing phase, and an aliasing error between the force plate and video data.

The time characteristics of the net torque components for the joints of the right leg are depicted in Fig. 9. The largest magnitudes of the net torques occur in the sagittal plane. Note that the $M_y(t)$ characteristic in Fig. 9 is split into two parts with different scales for the net torque to emphasize the characteristics of the lower leg torques during the take-off phase. The negative sign of the torque in the hip and ankle joint, in the second half of the support phase, indicates a common action of the quadriceps and triceps surae muscles.

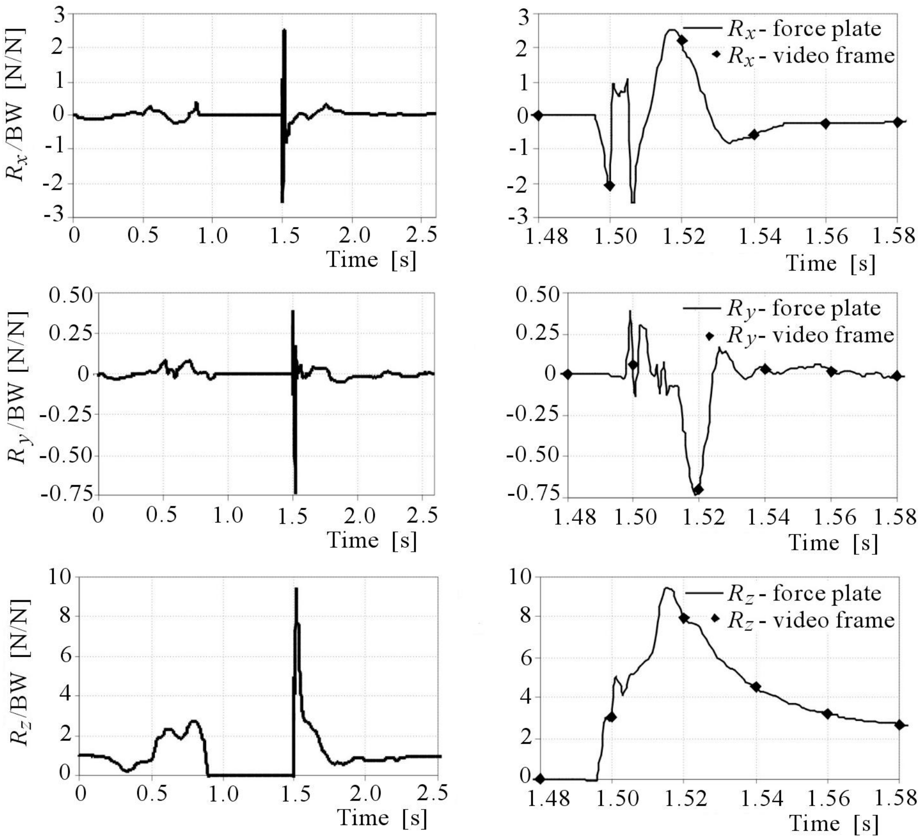

Fig. 8. Time-histories of the components of the ground reaction force measured in the force platform (left) and their expanded views during the beginning of landing (right). The markers denote the time instants for which there are video frames available

Just prior to the airborne phase, the net torque in the hip starts changing its direction anticipating a later movement of the thighs towards the trunk. The shapes of all curves for the net torques during flight are similar to those reported in the work by Blajer and Czaplicki (2001). The landing phase begins with a considerable load of the hip joint, changing rapidly from 6 Nm/BM (400 Nm) to more then −10 Nm/BM (−700 Nm). Such an instantaneous rise in the magnitude of the net torque cannot be done by the muscles alone. This impact seems to be conveyed by joints and ligaments and followed almost immediately by a strong action of the hip extensors like gluteus maximus, adductor magnus, semimembranosus and semitendinosus, and knee extensors. The results obtained during landing are qualitatively similar to those presented in the work of McNitt-Gray *et al.* (2001), where the landing phase of several different jumps, including backwards somersault, was subjected to a detailed dynamical analysis in a two-dimensional space.

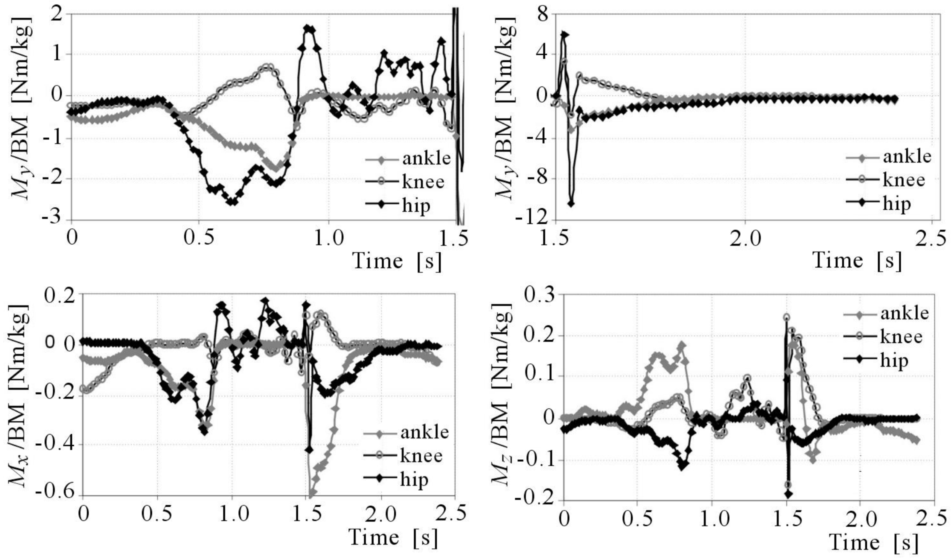

Fig. 9. Normalized net torques at the anatomical joints of the right leg of the jumper

The magnitudes of the net torque in the frontal and transversal plane are one order lower to those achieved in the sagittal plane. A remarkable eversion in the ankle joint at the beginning of landing is worth noticing. Simultaneously, the feet and the shank are rotated medially as a consequence of the fact that the jumper tries to hold his position standing on his fingers, as illustrated in Fig. 4b. Finally, there are also distinguishable net torque values in both planes during the second half of the supporting phase, which suggests the involvement of passive elements of the joints in these directions.

The results of identification of reaction forces in the selected joints in the case of the standing backwards somersault are shown in Fig. 10. It is clearly visible, when comparing the curves presented in Fig. 8 and Fig. 10, the remarkable damping of the vertical reaction between the ground and hip joint that ranges from 5 to 1.5 times the body weight. The shape of the vertical joint reaction during take-off and landing correspond closely to the shape of the ground reaction force. One should emphasize the positive signs of the vertical joint reaction at the beginning of the airborne phase and the considerable values of the anterior-posterior reaction in the hip joint, changing suddenly from 0.7 N/BW (466;) to more than −1.1 N/BW (−740 N) during the impact phase of landing.

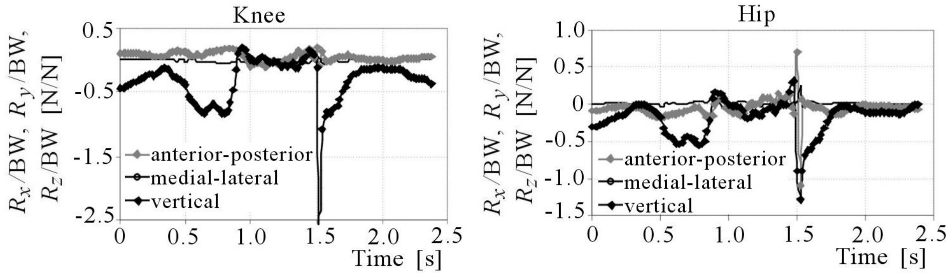

Fig. 10. Normalized reaction forces in the selected joints of the right leg during the standing backwards somersault

6. Conclusions

In the present work a general three-dimensional multibody methodology for calculating the net torques and reactions in joints has been demonstrated. The methodology consists of a biomechanical model, data acquisition techniques and an inverse dynamics analysis procedure integrated in a compact software package. The biomechanical model of the human body is constructed with rigid bodies interconnected by revolute and universal joints using the benefits of a general multibody formulation based on natural coordinates, well suited to define rigid bodies and kinematic joints and to a direct mapping between anatomical landmarks and body coordinates.

The biomechanical model is controlled by joint and driver actuators. The Lagrange multipliers assigned to all driver actuators effectively represent internal forces in the joints of the biomechanical model, either due to reaction forces or net moment of forces. The solution to the problem of inverse dynamics is unique and non-redundant, but it should be emphasized that the joint reactions obtained this way are underestimated.

The application of the methodology developed to a long jump and a standing backwards somersault allows the identification of the internal forces acting in the joints of the biomechanical model of the human body. The results have been explained in terms of their relevance to both investigated motor tasks. The results precisely reflect the impulsive nature of motions studied through its consequences in the shape of curves of the torques and reaction forces. However, some care must be taken when interpreting the results because they are sensitive to the procedure of smoothing the kinematic data. It also seems to be important to collect a large number of video frames, particularly during the supporting and landing phase of the motion. The obtained net torques may be used as the input data to solve an individual muscle distribution problem by means of adequate optimization methods, which in turn allows one to compute "real" reactions in the joints. The answer of which loads, and in which direction cross the joints during these activities may be of considerable interest to clinicians and trainers.

Acknowledgments

The support of this work by The Fundaçao para e Ciencia e Tecnologia, through the project EME/399976/Z, is gratefully acknowledged. The raw data for the presented study has been collected at The Faculty of Human Kinetics with the support by Dr. Orlando Jesus and Prof. Joao Abrantes, to whom the authors are grateful.

References

1. Abdel-Aziz Y., Karara, H., 1971. Direct linear transformation from comparator co-ordinates into object space co-ordinates, *Proc. ASP/UI Symposium on Close-Range Photogrammetry*, 1-18
2. Ambrósio J., Abrantes J., Lopes G., 2001, Spatial reconstruction of human motion by means of a single camera and a biomechanical model, *Human Movement Science*, **20**, 829-851
3. Blajer W., Czaplicki A., 2001, Modeling and inverse simulation of somersaults on the trampoline, *Journal of Biomechanics*, **34**, 12, 1619-1629
4. Blajer W., Czaplicki A., 2003, Contact modeling and identification of planar somersaults on the trampoline, *Multibody System Dynamics*, **10**, 289-312
5. Bobbert M., van Schenau G., 1988, Coordination in vertical jumping, *Journal of Biomechanics*, **21**, 3, 249-262
6. Celigüeta J.T., 1996, Multibody simulation of human body motion in sports, *Proc. XIV International Symposium on Biomechanics in Sports*, 81-94
7. Eberhard P., Spägele T., Gollhofer A., 1999, Investigations for the dynamical analysis of human motion, *Multibody System Dynamics*, **3**, 1-20
8. Haug E., 1989, *Computer Aided Kinematics and Dynamics of Mechanical Systems*, Allyn and Bacon, Boston

9. Hay J.G., 1993, Citius, altius, longius (faster, higher, longer): the biomechanics of jumping for distance, *Journal of Biomechanics*, **26**, Suppl. 1, 7-21

10. Jalón, J., Bayo E., 1994, *Kinematic and Dynamic Simulation of Multibody Systems: the Real-Time Challenge*, Springer-Verlag, New York

11. Jalón J.G., Unda, J., Avello A., 1986, Natural coordinates for the computer analysis of multibody systems, *Computer Methods in Applied Mechanics and Engineering*, **56**, 309-327

12. Laananen D., 1991, Computer Simulation of an Aircraft Seat and Occupant in a Crash Environment, Program SOM-LA/SOM-TA, DOT/FAA/CT-90/4, US Department of Transportation, Federal Aviation Administration

13. Laananen D., Bolukbasi A., Coltman J., 1983, Computer Simulation of an Aircraft Seat and Occupant in a Crash Environment - Volume 1, Technical report DOT/FAA/CT-82/33-I, US Department of Transportation, Federal Aviation Administration

14. Lees A., Smith P.G., Fowler N.E., 1994, A biomechanical analysis of the last stride, touchdown and takeoff characteristics of the men's long jump, *Journal of Applied Biomechanics*, **10**, 61-78

15. McNitt-Gray J.L., Hester D.M.E., Mathiyakom W., Munkasy B.A., 2001, Mechanical demand and multijoint control during landing depend on orientation of the body segments relative to the reaction force, *Journal of Biomechanics*, **34**, 1471-1482

16. Mieczkowski T., 1982, *Akrobatics*, WSP, Szczecin (in Polish)

17. Nikravesh P., 1988, *Computer-Aided Analysis of Mechanical Systems*, Prentice-Hall, Englewood Cliffs

18. Pandy M.G., Anderson F.C., Hull D.G., 1992, A parameter optimization approach for the optimal control of large-scale musculoskeletal systems, *Journal of Biomechanical Engineering*, **114**, 450-460

19. Pandy M., Zajac F., Sim E., Levine W., 1990, An optimal control model for maximum-height human jumping, *Journal of Biomechanics*, **23**, 12, 1185-1198

20. Schiehlen W., 1997, Multibody system dynamics: roots and perspectives, *Multibody System Dynamics*, **1**, 149-188

21. Selbie W.S., Caldwell G.E., 1996, A simulation study of vertical jumping from different starting postures, *Journal of Biomechanics*, **29**, 9, 1137-1146

22. Silva M., 2003, Human motion analysis using multibody dynamics and optimization tools, Ph.D. Thesis, Technical University, Lisbon

23. Silva M., Ambrósio J., 2002, Kinematic data consistency in the inverse dynamic analysis of biomechanical systems, *Multibody System Dynamics*, **8**, 219-239

24. Silva M., Ambrósio J., Pereira M., 1997, Biomechanical model with joint resistance for impact simulation, *Multibody System Dynamics*, **1**, 65-84

25. Winter D.A., 1990, *Biomechanics and Motor Control of Human Movement*, John Wiley and Sons, New York

26. Zatsiorsky V.M., 1998, *Kinematics of Human Motion*, Human Kinetics, Champaign

Biomechaniczne modelowanie trójwymiarowych ruchów człowieka w środowisku współrzędnych naturalnych

Streszczenie

W pracy zaprezentowano pełną metodologię do badania ruchów człowieka. Podstawowym elementem tej metodologii jest trójwymiarowy biomechaniczny model ciała ludzkiego. Położenia członów modelu opisano za pomocą współrzędnych naturalnych, co wyeliminowało konieczność użycia współrzędnych kątowych. Model składa się z 33 ciał sztywnych połączonych przegubami (stawami) i posiada 44 stopnie swobody. Wypadkowe momenty sterujące w poszczególnych stawach pochodzące od sił mięśniowych wprowadzono do dynamicznych równań ruchu modelu za pomocą stosownych więzów kinematycznych pomiędzy sąsiadującymi członami w danym stawie. Wartości tych momentów wyznaczono wykorzystując formalizm mnożników Lagrange'a. Model wykorzystano do identyfikacji wypadkowych momentów mięśniowych i reakcji wewnętrznych w głównych stawach kończyny dolnej człowieka podczas odbicia do skoku w dal oraz w trakcie wykonywania salta w tył z miejsca.

Manuscript received March 19, 2004; accepted for print April 15, 2004